13.5 mJ polarized 2.09 μm fiber-bulk holmium laser and its application to a mid-infrared ZnGeP₂ optical parametric oscillator

Encai Ji (吉恩才), Mingming Nie (聂明明), and Qiang Liu (柳 强)*

State Key Laboratory of Precision Measurement Technology and Instruments, Department of
Precision Instrument, Tsinghua University, Beijing 100084, China
*Corresponding author: qiangliu@mail.tsinghua.edu.cn

A high pulse repetition frequency (PRF), high energy Ho:YAG laser directly pumped by a Tm-doped fiber laser and its application to a mid-infrared ZnGeP₂ (ZGP) optical parametric oscillator (OPO) is demonstrated. The maximum polarized 2.09 μm laser pulse energy is 13.46 mJ at a PRF of 1 kHz. The corresponding peak power reaches 504 kW. In a double-resonant ZGP-OPO, a maximum mid-infrared laser pulse energy of 1.25 mJ, corresponding to a peak power of 79 kW, is accomplished at a PRF of 3 kHz. The nonlinear conversion efficiency reaches 41.7%. The nonlinear slope efficiency reaches 53.3%.

OCIS codes: 140.3070, 140.3540, 140.4480, 140.5680, 190.4970.
doi: 10.3788/COL201715.091402.

The 2–5 μm pulsed lasers with a relative high pulse repetition frequency (PRF) and high pulse energy are of great value for scientific and technical applications, such as laser medical diagnostics, lidar systems, spectroscopy, and mid-infrared countermeasures[1–5]. In our previous work[6], a maximum 2.09 μm pulse energy of 12.8 mJ was reported at a PRF of 1 kHz with a Tm-doped fiber laser (TDFL) pumped Ho:YAG oscillator, which was nonpolarized. In addition, the element layer in the Ho:YAG cavity was easy to damage for the current coating technique. A larger pump spot size or master oscillator power amplifier (MOPA) can be utilized to further scale the pulse energy. To develop a mid-infrared laser with the frequency down conversion technique, a polarized fundamental wave needs to be well prepared in advance. In 2000, Budni *et al.*[7] introduced a Ho:YAG laser in the ZnGeP₂ (ZGP) optical parametric oscillator (OPO) system. A maximum mid-infrared pulse energy of 0.42 mJ at a PRF of 10 kHz was obtained with a peak power of 16.2 kW, but the fundamental laser was all solid-state, in which the laser output power with good beam quality was difficult to scale up because of the severe thermal load. Recently, a Tm-fiber-Ho-bulk cascaded laser has been widely used as the fundamental laser source of high PRF mid-infrared ZGP-OPO[8–10], mostly due to a better way of thermal management. In 2006, Lippert *et al.*[8] first presented this type OPO system and obtained mid-infrared pulse energy of 0.26 mJ at 20 kHz. They improved the pulse energy to about 0.49 mJ at 45 kHz in 2010 with a V-shaped ring OPO resonator[9]. In 2013, Hemming *et al.*[10] obtained the current maximum pulse energy of 1.16 mJ at a PRF of 26 kHz with a four-mirror ring OPO resonator. These fiber-bulk ZGP-OPO systems all aimed to obtain high average power at high PRF. To develop the mid-infrared ZGP-OPO with high pulse energy at high PRF,

there are few reports. Recently, new types of 2 μm mode-locking materials, such as layered metal dichalcogenides[11] and MoS₂[12], may be utilized to obtain a picosecond fundamental pulse with high peak power. But, the current pulse energy is limited. Therefore, our main task is to develop a high energy, high PRF mid-infrared ZGP-OPO with a TDFL-pumped Ho:YAG laser.

In this Letter, a high energy, high PRF polarized 2.09 μm Ho:YAG laser pumped by a homemade TDFL was first described. Then, the double-resonant ZGP-OPO was presented with this fundamental laser source. The maximum output 2.09 μm laser energy reached about 13.5 mJ at a PRF of 1 kHz, corresponding to continuous wave (CW) power of 16.7 W. The maximum 3–5 μm laser energy reached about 1.25 mJ at a PRF of 3 kHz, corresponding to the peak power of 71.6 kW.

Figure 1 shows the experimental setup of fiber-bulk fundamental laser. The pump source of the oscillator stage and amplifier stage are both homemade TDFLs with 100-W-level output power. The structure of TDFLs
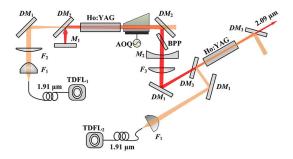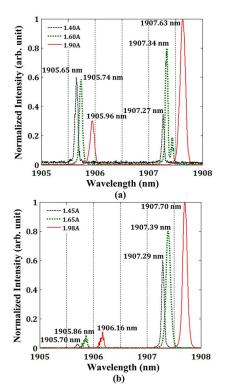

Fig. 1. Layout of the TDFL-pumped Ho:YAG oscillator and amplifier system. (DM₁, HT at 0.79 μm and HR at 1.91 μm; DM₂, HT at 1.91 μm and HR at 2.09 μm; DM₃, HT at *p*-polarized 2.09 μm and HR at 1.91 μm.)

(TDFL$_1$ and TDFL$_2$) is same as Ref. [5]. With a pair of convex lens (F_1 and F_2), the pump beam from TDFL$_1$ is collimated into the Ho:YAG crystal of the oscillator stage with a spot diameter of about 0.6 mm. Different from the oscillator structure in Ref. [5], a Brewster's angle thin film plate polarizer (BPP) is inserted before the output mirror (M_2) to merely resonate the p-polarized light, the Ho:YAG crystal is 0.7 at.%-doped, and the cavity geometric length is 250 mm. The pulse operation was accomplished with an acousto-optic Q-switch (AOQ, I-QS027-2.5C10V5-U5-ST3, Gooch & Housego). With one convex lens (F_1), the pump beam from TDFL$_2$ is collimated into the Ho:YAG crystal of the amplifier stage with a spot diameter of about 0.8 mm. Meanwhile, the seed laser from the oscillator stage is focused into the amplifier stage with a convex lens (F_3). The seed laser spot diameter in the amplifier crystal is about 0.6 mm. The size of the two crystals has a cross-section diameter of 4 mm and length of 7 cm.

The spectra of the TDFLs were first measured with a high-resolution spectral analyzer (AQ6375, Yokogawa). Figure 2(a) shows three typical output spectra of TDFL$_1$ when the pump current was set at 1.60, 1.90, and 2.20 A, respectively. The common feature for them is that a severe side mode, around 1905.8 nm, exits on the left of the expected main mode, around 1907.4 nm. This feature resulted in the almost zero output of the Ho:YAG laser. The Ho:YAG laser output came back to normal only with a little offset of the pump currents.

In addition, the lasing wavelength of the TDFL becomes larger at higher pump power, mostly due to the temperature rise of the fiber Bragg gratings (FBGs, ITF). Figure 2(b) shows three other spectra of TDFL$_1$ at 1.65, 1.95, and 1.98 A, respectively. The side mode becomes weak in comparison with that in Fig. 2(a). The corresponding CW output power was 1.67, 3.66, and 5.64 W, respectively. Finally, seven pump currents of TDFL$_1$ were chosen as the working points of the Ho:YAG oscillator experiment, and five pump currents of TDFL$_2$ were chosen as the working points of the Ho:YAG amplifier experiment.

The main CW output characteristics of the Ho:YAG oscillator were shown in Fig. 3. The pump absorption efficiency of the Ho:YAG in the lasing condition was >97% without the element of BPP (η_1), but it decreased to about 94.2% with BPP (η_2). The maximum CW nonpolarized output power of 14.86 W, as shown by P_{s1} in Fig. 3(a), was achieved at the pump power of 59.7 W, corresponding to an optical-to-optical efficiency of 24.9%. By inserting BPP, the maximum CW-polarized output power was 9.25 W, as shown by P_{s2} in Fig. 3(a). The polarized efficiency was about 62.25% relative to the nonpolarized output case. Compared with the efficiency in previous work[6], here, the low conversion efficiency was mainly due to the low spectral purity of TDFL$_1$. The transmittance of dichroic mirror DM$_3$ was > 95%, as shown by T_{DM3} in Fig. 3(a). Figure 3(b) depicts the beam quality and the
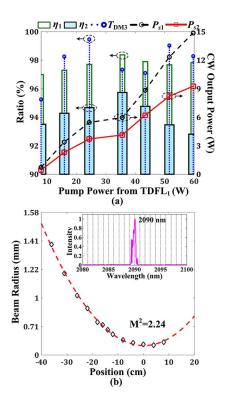

Fig. 2. (Color online) Typical output spectra of TDFL$_1$. (a) The pump current was set at 1.40, 1.60, and 1.90 A, respectively; (b) the pump current was set at 1.45, 1.65, and 1.98 A, respectively.

Fig. 3. (Color online) CW output characteristics of polarized the Ho:YAG oscillator. (a) The pump absorption efficiency of the Ho:YAG crystal, the CW output power, and the transmittance of DM$_3$; (b) the beam quality measurement and spectrum of the output laser.

spectrum of the output laser at the maximum-polarized output case. With the 90/10 knife-edge method, the beam quality factor, $M^2 = 2.24$, was obtained. The central lasing wavelength was 2090 nm, as shown in the inset picture of Fig. 3(b).

The main Q-switched output characteristics of the Ho:YAG oscillator were shown in Fig. 4, corresponding to the CW-polarized output power of 8.42 W. A maximum pulse energy of 6.42 mJ was obtained at a PRF of 1 kHz, as shown in Fig. 4(a). The Q-switched efficiency was about 78.3%. The pulse energy decreased to about 0.162 mJ at a high PRF of 50 kHz, corresponding to a Q-switched efficiency of 96.2%. Meanwhile, the pulse duration increased linearly from 24.03 to 413.7 ns with a slope ratio of 8.10 ns/kHz. Figure 4(b) also depicts the typical pulse profiles in eight different PRFs, which basically follow the Gaussian distribution. The pulse duration becomes narrower at a lower PRF, which is mainly caused by the sharp rise of the initial population inversion and the decrease of the final population inversion.

The DM_1 mirror after F_3 in Fig. 1 was placed with an incident angle of 30° to maximally reflect the p-polarized 2.09 μm laser. Under the condition of the CW seed input, the output power of the amplifier stage was shown in Fig. 5(a). The maximum output was basically obtained with a pump power of 37 W for different seed powers. The maximum CW-polarized output power of 16.68 W was finally accomplished with the seed power of

Fig. 5. (Color online) Output characteristics of the polarized Ho: YAG amplifier. (a) Amplified output CW power versus pump power from $TDFL_2$; (b) amplifier pulse energy and pulse duration versus PRF with $TDFL_1$ power of 51.6 W and $TDFL_2$ power of 37 W.

8.05 W. The total optical-to-optical efficiency was about 20.75%. The Ho:YAG crystal of the amplifier stage exhibits an obvious absorption loss for the 2.09 μm laser. It reached $>80\%$ with the seed power of $<1W$, but dramatically decreased to about 43% with the seed power of 8.05 W. Thus, there is a pump threshold for the effective energy extraction of a quasi-three-level Ho:YAG amplifier. In our experiment, the transparency pump threshold was around 20 W, as shown in Fig. 5(a). Under the condition of pulsed seed input, the output pulse energy and pulse duration of the amplifier stage were shown in Fig. 5(b) with a pump power of 37 W. A maximum pulse energy of 13.46 mJ was obtained at a PRF of 1 kHz, corresponding to the seed energy of about 6.3 mJ. The pulse duration and peak power were 26.69 ns and 504 kW, respectively. The total optical-to-optical efficiency was about 15.19%.

In the experiments above, the Ho:YAG laser performance was of value for the study of the mid-infrared non-linear process. Here, we apply this fiber-bulk holmium laser system to ZGP-OPO to obtain a 3–5 μm pulsed laser. Figure 6 illustrates the experimental layout of the mid-infrared ZGP-OPO. The double-resonant OPO cavity was structured with two plane mirrors (M_3 and M_4), which were all placed with a small tilt angle to prevent the bad effect of laser feedback on the pump source and weaken the reverse process of OPO[13,14]. Output mirror M_4 has a high pump transmittance of 90% and a parametric transmittance of 50%. Thus, it was almost a single-pass
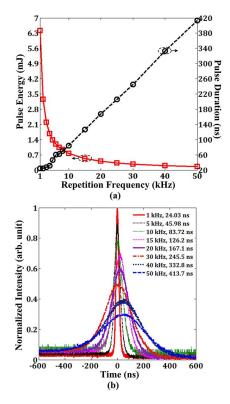

Fig. 4. (Color online) Pulsed output characteristics of the polarized Ho:YAG oscillator. (a) Pulse energy and pulse duration versus PRF with pump power of 51.6 W; (b) the pulse profiles at eight different PRFs.
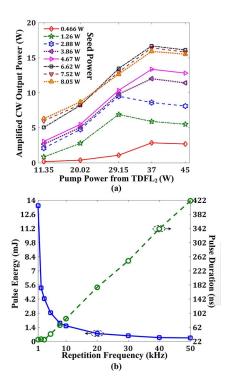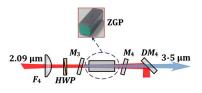
Fig. 6. Layout of the TDFL-pumped Ho:YAG oscillator and amplifier system. (DM$_4$, $T \approx 90\%$ at 3–5 μm and HR at p-polarized 2.09 μm).

pumping scheme. A half-wave-plate (HWP) was inserted before the cavity to rotate the polarization direction to obtain the perfect phase match. The ZGP crystal was wrapped with indium foil and naturally cooled through a copper heat sink at room temperature. The phase matching angles $\theta = 55.5°$, $\psi = 0°$ of I-type ZGP were designed to obtain nearly degenerate mid-infrared light. The size of the ZGP crystal was 6 mm × 6 mm × 18 mm. Another dichroic mirror, DM$_4$, was adopted to filter the residual pump light. About 10% of the parametric power was lost by DM$_4$. The pump pulse and parametric pulse were simultaneously detected with an InGaAs detector and a PbSe detector.

The ZGP-OPO was first pumped with the pulsed output laser of the Ho:YAG oscillator. The focal length of lens F_4 was 250 mm. The collimated pump spot diameter was about 0.75 mm. In the PRF range of 1–7 kHz and cavity length range of 4–8 cm, the parametric pulse energy was measured in detail. The result indicated the maximum output pulse energy was obtained at a PRF of 3 kHz and cavity length of 4 cm. With an input pump energy of 1.77 mJ at a PRF of 3 kHz, the output parametric pulse energy was about 0.363 mJ with a pulse duration of 14.67 ns, which was much less than the pump pulse duration of 27.6 ns, as shown in Fig. 7(a). The pump pulse intensity was calculated as 0.4 J/cm^2. The conversion efficiency was about 22.8% in consideration of the loss of DM$_4$. The parametric pulse building time was about 14.85 ns with the definition in Ref. [15]. The parametric pulse rising time was about 7.7 ns with the definition in Ref. [16]. The beam quality factor, $M^2 = 2.545$, was obtained, as shown in Fig. 7(b). A low resolution spectral analyzer (SM301-EX, Spectral Products) was adopted to roughly estimate the parametric wavelength. The central wavelengths of the resonant signal light and idler light were around 3.9 and 4.5 μm with the maximum output of 0.363 mJ. The line width was not accurately estimated because of the resolution of > 150 nm around 4 μm. The minimum central signal wavelength can be tuned to around 3.5 μm by rotating ZGP, but the output energy decreased to about 0.2 mJ. The central signal wavelength can also be increased by rotating ZGP in the inverse direction. The output energy decreased to zero around 4 μm and 0.1 mJ around 4.18 μm.

To further scale the mid-infrared pulse energy and the conversion efficiency, the ZGP-OPO was then pumped with the pulsed output laser of the Ho:YAG amplifier.
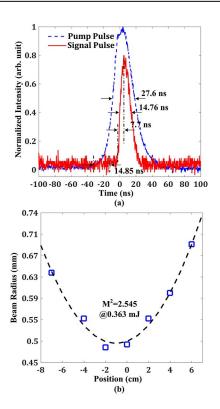

Fig. 7. (Color online) (a) Comparison of typical pump pulse profile and parametric pulse profile; (b) the beam quality measurement of parametric light.

The focal length of lens F_4 was now 200 mm. The collimated pump spot diameter was about 0.70 mm. The maximum incident pump energy was about 3 mJ at a PRF of 3 kHz, corresponding to a pulse intensity of 0.78 J/cm^2, which was far less than the damage threshold of about 2 J/cm^2[17–19]. Figure 8 shows the main output characteristics in such a case. The experimental maximum output parametric average power was 3.38 W with a pulse duration of 15.82 ns. The slope efficiency was fitted as 53.29%, as shown in Fig. 8(a). Considering the loss of DM$_4$, the actual parametric pulse energy was 1.252 mJ at a PRF of 3 kHz, corresponding to a peak power of 79.13 kW and a conversion efficiency of 41.73%. The parametric conversion in this work has exceeded the maximum value of 40.73% in Ref. [20], but was still far less than the theoretical maximum value of 81.45% in Ref. [13], which indicates that the reverse parametric conversion effect was partially inhibited, and the pump intensity was still less than the optimum value. Figure 8(b) depicts three typical beam quality measurements in output pulse energy of 0.37, 0.72, and 1.13 mJ, respectively. The beam quality degraded gradually along with the increase of output pulse energy. The beam quality factor, $M^2 = 3.759$, was obtained in the case of maximum output pulse energy.

In conclusion, the maximum polarized 2.09 μm CW power of 16.7 W and polarized 2.09 μm pulse energy of 13.46 mJ at a PRF of 1 kHz are achieved in a TDFL-pumped Ho:YAG laser. By applying this polarized 2.09 μm pulse laser to ZGP-OPO, the maximum
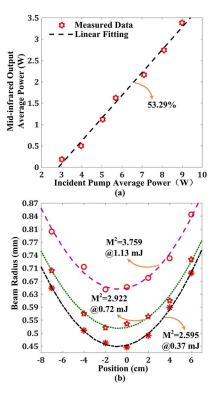
Fig. 8. (Color online) (a) Total parametric output average power versus incident pump average power at a PRF of 3 kHz; (b) the beam quality measurements at three typical parametric pulse energies.

3–5 μm pulse energy of 1.25 mJ at a PRF of 3 kHz is achieved with a conversion efficiency of 41.73% and a slope efficiency of 53.29%. The peak power reaches about 79.13 kW. The parametric pulse energy and conversion efficiency can be further improved by increasing the pump intensity.

References

1. J. Wu, Y. Ju, B. Yao, T. Dai, Z. Zhang, X. Duan, and Y. Wang, Chin. Opt. Lett. **15**, 031402 (2017).
2. F. K. Tittel, R. Lewicki, M. Jahjah, B. Foxworth, Y. F. Ma, L. Dong, R. Griffin, K. Krzempek, P. Stefanski, and J. Tarka, in *Terahertz and Mid Infrared Radiation: Detection of Explosives and CBRN (Using Terahertz)* (Springer, 2014), p. 153.
3. O. Henderson-Sapir, J. Munch, and D. J. Ottaway, Opt. Lett. **39**, 493 (2014).
4. E. Lippert, G. Rustad, G. Arisholm, and K. Stenersen, Opt. Express **16**, 13878 (2008).
5. R. J. De Young and N. P. Barnes, Appl. Opt. **49**, 562 (2010).
6. E. Ji, Q. Liu, Z. Hu, P. Yan, and M. Gong, Chin. Opt. Lett. **13**, 121402 (2015).
7. P. A. Budni, L. A. Pomeranz, M. L. Lemons, C. A. Miller, J. R. Mosto, and E. P. Chicklis, J. Opt. Soc. Am. B **17**, 723 (2000).
8. E. Lippert, S. Nicolas, G. Arisholm, K. Stenersen, and G. Rustad, Appl. Opt. **45**, 3839 (2006).
9. E. Lippert, H. Fonnum, G. Arisholm, and K. Stenersen, Opt. Express **18**, 26475 (2010).
10. A. Hemming, J. Richards, A. Davidson, N. Carmody, N. Simakov, M. Hughes, P. Davies, S. Bennetts, and J. Haub, in *Conference Lasers and Electro-Optics* (2013), p. 1.
11. H. R. Yang and X. M. Liu, Appl. Phys. Lett. **110**, 171106 (2017).
12. L. C. Kong, G. Q. Xie, P. Yuan, L. J. Qian, S. X. Wang, H. H. Yu, and H. J. Zhang, Photon. Res. **3**, A47 (2015).
13. G. Breitenbach, S. Schiller, and J. Mlynek, J. Opt. Soc. Am. B **12**, 2095 (1995).
14. B. Q. Yao, J. H. Yuan, J. Li, T. Y. Dai, X. M. Duan, Y. J. Shen, Z. Cui, and Y. B. Pan, Opt. Lett. **40**, 348 (2015).
15. S. Brosnan and R. Byer, IEEE J. Quantum Electron. **15**, 415 (1979).
16. J. Pearson, U. Ganiel, and A. Yariv, IEEE J. Quantum Electron. **8**, 433 (1972).
17. R. D. Peterson, K. L. Schepler, J. L. Brown, and P. G. Schunemann, J. Opt. Soc. Am. B **12**, 2142 (1995).
18. K. T. Zawilski, S. D. Setzler, P. G. Schunemann, and T. M. Pollak, J. Opt. Soc. Am. B **23**, 2310 (2006).
19. A. Hildenbrand, C. Kieleck, A. Tyazhev, G. Marchev, G. Stoppler, M. Eichhorn, P. G. Schunemann, V. L. Panyutin, and V. Petrov, Opt. Eng. **53**, 122511 (2014).
20. J. Bjorkholm, IEEE J. Quantum Electron. **7**, 109 (1971).